TRIANGULATION OF SPACEBORNE THREE-LINE ARRAY IMAGERY WITH DIFFERENT SENSOR MODELS

Yongjun Zhang[1, 2]
Maoteng Zheng[1]
Tao Ke[1]
1. School of Remote Sensing and Information Engineering
Wuhan University
Wuhan, 430079, China
zhangyj@whu.edu.cn
tengve@163.com
2. State Key Laboratory of Information Engineering in Surveying, Mapping and Remote Sensing,
Wuhan 430079, China
zhangyj@whu.edu.cn

ABSTRACT

Spaceborne linear array sensors have been introduced into photogrammetry since more than twenty years ago. The traditional solution of frame photograph cannot deal with image data of linear array sensor anymore, because the position and attitude of the spacecraft vary at each scanner line. Thus the number of unknowns would be extremely large and it is impossible to determinate the exterior orientation parameters of each scanner line. A proper approximation has to be applied to model the spacecraft trajectory to reduce the unknowns in triangulation. There are three models feasible to represent the satellite trajectory: Quadratic Polynomial Model (QPM), Systematic Error Compensation Model (SECM), and Orientation Image Model (OIM). Revealing the differences of the three sensor models and relationships between different control strategies and the final accuracy of georeferencing after bundle adjustment is the main purpose of this paper. To fully evaluate the accuracy that spaceborne three-line scanner can achieve, experiments with LMP, SECM and OIM triangulation algorithms are performed with a 500km length data sets under WGS 84 coordinate system.

KEYWORDS: Three-line Array Imagery, Triangulation, Trajectory Model, Precision Analysis

INTRODUCTION

Three-line array image technology is first proposed by Hoffman (Hoffman, 1982). Owing to the pushbroom scanning strategy with three linear arrays, the problem of small image format of traditional aerial image is solved. The base-height ratio is also increased largely, which could improve the altitude accuracy. It has been successfully applied in MOMS satellite, and satisfactory results have been obtained (Ackermann, 1990; Ebner, 1991a; Ebner, 1991b; Ebner, 1992). The design of three-line array pushbroom scanner is also adopted by SPOT5 satellite, with two HRS cameras tilted by ±20degrees, the maximum base-height ratio is 0.8, and the GSD is 10m across track and 5m along track. The nadir looking panchromatic HRG instrument provides imagery at 5m GSD in the mono-spectral bands HMA and HMB, the ground pixel scenes of which are interleaved and shifted 2.5m in order to obtain the interpolation of so-called THR images (SPOT Image, 2002). It's a successful example of mapping with three-line array images. ALOS Prism is another three-line array satellite sensor that has been widely applied in mapping applications (Gruen et al., 2007).

In recent years, with the development of the civil surveying satellites, particularly the successful launching of CBERS-01 and CBERS-02, the techniques of earth-observation and stereo mapping in China have been promoted greatly. CBERS-02 is the first high resolution earth observation satellite in our country, on which the single linear pushbroom scanner is adopted and 2.36m ground resolution HR camera is carried (Yue et al., 2009; Yu, 2008). Whereas the ERS-III scheduled to be launched in 2012, is designed for three-line array pushbroom scanning. The tilted angles are ±22 degrees, so the maximum intersection angle is 44 degrees. The GSD of nadir, foresight, and back sight are about 2.1m, 3.5m and 3.5m, respectively. However, because of the disparities in hardware, the accuracies of direct georeferencing are lower than that of the advanced countries. As to CBERS-02, the desired accuracy is 50m, but the actual accuracy is usually on the several hundred meters level, unless the image is divided

into short orbit data and processed with certain GCPs. To deal with orientation of large area data, spatial triangulation combined with position and attitude observations has to be implemented. Previous experiments indicate that the accuracy could achieve 1-2 GSD after triangulation with a few GCPs distributed evenly around the area.

There are a lot of works have been done in photogrammetric applications (generating the DEM, DOM etc) with space-borne three-line CCD images. In order to generate photogrammetric products, we have to establish the mathematical relationship between image space and object space first. Most of the models can be classified into two types: Rigorous Physical Model and General Model (McGlone, 1996). General model is actually using a rational function to describe the relationship between image space and object space such as RFM (Tao and Hu, 2001; Dial, 2002). In Rigorous Physical Model, Exterior Orientation Parameters (EOPs) are usually adopted to represent the position and attitude of the sensor, collinearity equations is the basic mathematical model. It's a relatively strict sensor model (Tao and Hu, 2001). And it will be adopted in this paper to reconstruct the geometry relationship between image and object space. In common sense, the number of line images is quite large, which makes it unable to directly solve all these EOPs simultaneously during triangulation (Zhao and Li, 2006). A trajectory model has to be applied to describe the changing of satellite's position and attitude while scanning. Usually, Quadratic Polynomial Model (QPM), Systematic Error Compensation Model (SECM), Piecewise Polynomial Model (PPM) and Orientation Image Model (OIM) are used. Many researchers have worked on these models (Ohlhof, 1995; Zhao and Li, 2006), but few of them have specifically compared the performance of these models with the same dataset. In this paper, experiments of triangulation with ~~LMP,~~ SECM and OIM are performed with a 500km length dataset under WGS 84 coordinate system to evaluate the three models and to investigate the relationship between the number of GCPs used in triangulation and the achieved accuracy.

MATHEMATICAL MODEL OF ADJUSTMENT

To decrease the number of unknowns, a trajectory model has to be used. Jung had developed a stochastic model based on the first order Gauss Markov process (Jung, 2008). General trajectory model includes QPM, SECM and OIM. QPM is very simple, but only designed for data of short orbit which can be fitted by a polynomial. As the orbit gets longer, this model is unable to represent the changing of position and attitude of satellite. SECM can be applied to model longer orbit data. However, when the orbit length is more than 1,000km, the suitable solution is OIM, which was first proposed by Hoffman (Hoffman, 1982). After that, this model had been widely used in processing of both spatial and aerial linear CCD images.

Quadratic Polynomial Model (QPM)

As demonstrated by the equations below, each exterior orientation parameter (EOP for short) can be represented by a quadratic polynomial about time.

$$Xs = a_0 + a_1 t + a_2 t^2$$
$$Ys = b_0 + b_1 t + b_2 t^2$$
$$Zs = c_0 + c_1 t + c_2 t^2$$
$$\varphi = d_0 + d_1 t + d_2 t^2$$
$$\omega = e_0 + e_1 t + e_2 t^2$$
$$\kappa = f_0 + f_1 t + f_2 t^2$$

Systematic Error Compensation Model (SECM)

The relationship between EOP and time is described by the following equations:

$$Xs = Xs_0 + a_0 + a_1 t + a_2 t^2$$
$$Ys = Ys_0 + b_0 + b_1 t + b_2 t^2$$
$$Zs = Zs_0 + c_0 + c_1 t + c_2 t^2$$
$$\varphi = \varphi_0 + d_0 + d_1 t + d_2 t^2$$
$$\omega = \omega_0 + e_0 + e_1 t + e_2 t^2$$
$$\kappa = \kappa_0 + f_0 + f_1 t + f_2 t^2$$

In which, Xs_0, Ys_0, Zs_0, φ_0, ω_0, κ_0 are positions and attitudes of the satellite at time *t* which derived from observations obtained by the Globe Positioning System and Inertial Measure Unit on board.

Orientation Image Model (OIM)

Extract certain CCD lines as orientation images, the EOP of CCD lines between orientation images can be calculate by EOPs of CCD lines at the nearest four orientation images.

$$P(t_j) = \sum_{i=K-1}^{K+2} [P(t_i) \bullet \prod_{\substack{k=K-1 \\ k \neq i}}^{K+2} \frac{t - t_k}{t_i - t_k}]$$

In which, $P(t_j)$ and $P(t_i)$ represent the EOPs at time t_j and t_i.

Adjustment Process and Weight Strategy

For the OIM, the EOPs of all orientation images are solved directly. These EOPs including translation parameters and angular parameters which are referencing to geocentric coordinate system, and they are strongly related for spaceborne platforms (Kim and Dowman, 2006). In order to avoid the relativity between translation parameters and angular parameters, this experiment firstly makes a constant systematic error correction on position and attitude observations which can eliminate the drift errors of the entire orbits and then assumes that the translation parameters are known, so only three angular parameters of EOPs need to be solved in the bundle adjustment process. The interval of OIM is set to be 1,5000 scanning lines (the interval time is about 10 seconds). The weight of the observations of position and attitude are fixed during adjustment. The initial weights of image points are set to be 1.0 and the weights of others are set to be the square of the ratio of its accuracy against the accuracy of image point observations. After iteration during adjustment, the weight of each image point is recalculated according to its residues.

EXPERIMENTS AND ANALYSIS

Ground and image data of a spaceborne three-line CCD sensor is adopted for experiment. The tilted angles are ±25 degrees. Ground resolutions of all the three sights are 5m. The entire length of the orbit is more than 1,000km and the overlapped region of three images is about 500km. Evenly distributed pass points are automatically matched with about 0.3 pixels precision. GCPs are measured from old aerial orthophoto with 1:10,000 scales. Totally 58 points are measured. There are possible gross errors in these GCPs because the old aerial orthophoto was generated decades ago.

Most traditional adjustment technologies of satellite linear array images adopt three models: QPM, SECM and OIM. These three models are used to evaluate the abilities of eliminating systematic errors of each model and to investigate the relationship between the number of GCPs and the achieved accuracy. The orientation models, number of GCPs and check points (CKPs) used for experiments are listed as follows:

QPM	(a)	4 GCPs, 54 CKPs	(1)
SECM	(b)	8 GCPs, 50 CKPs	(2)
OIM	(c)	14 GCPs, 44 CKPs	(3)
		22 GCPs, 36 CKPs	(4)
		52 GCPs, 6 CKPs	(5)

Comparison of Three Trajectory Models

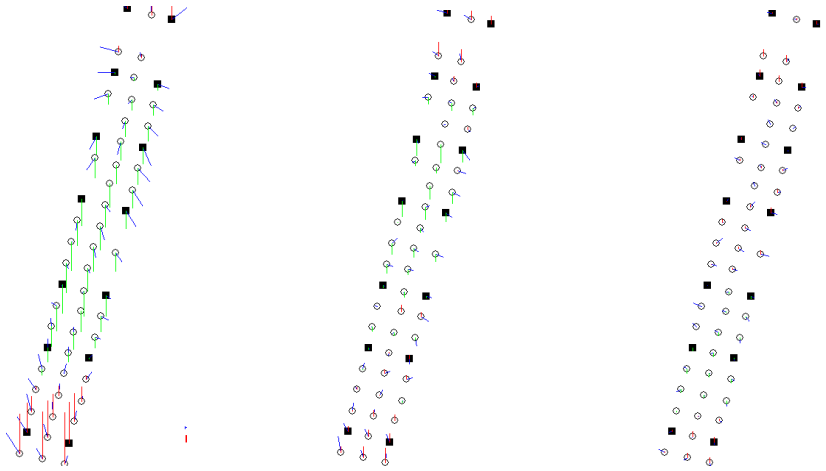

Figure 1. Absolute errors of control and check points of QPM, SECM and OIM (a) by control strategies (3). The black squares are control points, the white circle check points, red lines positive Height RMS, Green lines minus Height RMS, blue lines Planar RMS. The length of the lines represent the values of RMSs.

Table 1. Error statistics of check points after triangulation whit three models

Model	Check Points RMS	(3)		
		X	Y	Z
QPM	MEAN(m)	-1.29	0.44	-9.06
	STDEV(m)	11.16	17.80	36.66
	MAX(m)	32.13	34.69	85.39
	MIN(m)	0.26	0.87	1.35
SECM	MEAN(m)	0.88	1.65	-1.96
	STDEV(m)	7.46	8.68	13.68
	MAX(m)	14.15	27.59	32.04
	MIN(m)	0.14	0.08	0.64
OIM	MEAN(m)	-0.35	0.53	1.01
	STDEV(m)	4.87	2.00	7.93
	MAX(m)	15.60	10.92	11.93
	MEAN(m)	0.03	0.17	0.10

As showed in Figure 1 and Table 1, QPM had the worst result as compared to the other two models after triangulation with the same control strategy (14 control points, 44 check points). SECM can achieve better result than QPM but worse than OIM which was known to be the most appropriate model to deal with spaceborne image data of long orbit.

Triangulated Results of QPM with Different Control Strategies

Three control strategies (1, 3, 5) were applied.

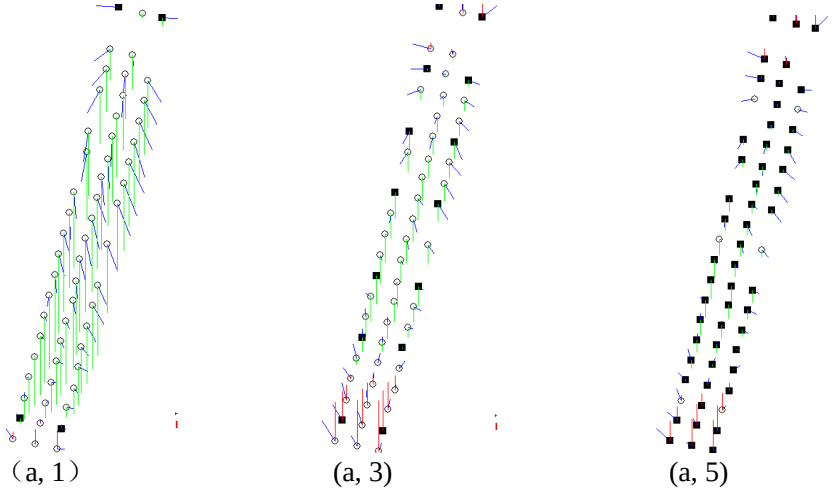

Figure 2. Absolute errors of control and check points of QPM (a) by control strategies (1), (3), (5).

Table 2. Error statistics of check points **of** triangulat**ed results** with **QPM**

CKPs RMS	(1)			(3)			(5)		
	X	Y	Z	X	Y	Z	X	Y	Z
MEAN(m)	5.2	-27.6	-87.5	-1.3	0.4	-9.1	0.7	0.9	-1.8
STDEV(m)	11.9	21.2	43.3	11.2	17.8	36.7	15.3	12.6	20.5
MAX(m)	29.4	60.7	134.0	32.1	34.7	85.4	24.6	21.5	30.2
MIN(m)	0.2	1.0	2.1	0.3	0.8	1.3	3.7	0.4	4.0

From Figure 2 and Table 2, we find that the RMS of check points after triangulation using QPM decreases while the number of control points increases. But even using most of the given points as control, the maximum residue is 30.2m, which is unacceptable. In Figure 2(a,1), 2(a,3), 2(a,5), the changes of height RMS of control points and check points are relative to the time parameters, which means that this model causes a new type of systematic error. It fits the fact that fitting long orbit data with QPM is unreasonable.

Triangulated Results of SECM with Different Control Strategies

Three control strategies (1, 3, 5) were applied.

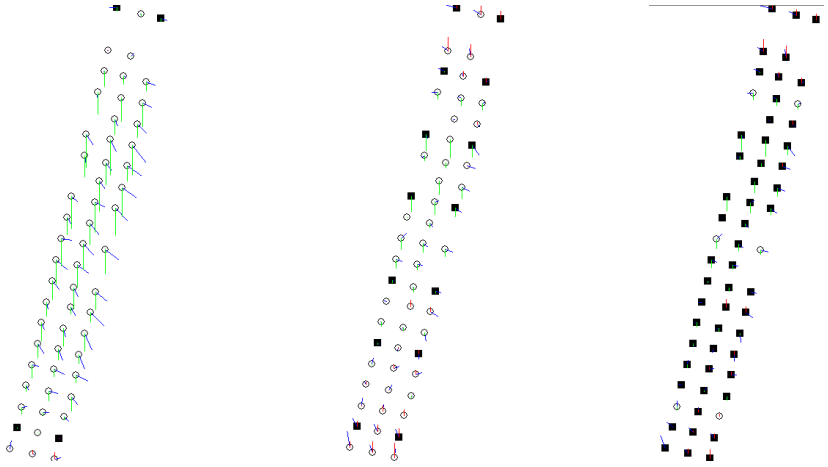

（b, 1） (b, 3) (b, 5)

Figure 3. Absolute errors of control and check points of SECM (b) by control strategies (1), (3), (5).

Table 3. Error statistics of check points of triangulated results with SECM

CKPs RMS	(1)			(3)			(5)		
	X	**Y**	**Z**	**X**	**Y**	**Z**	**X**	**Y**	**Z**
MEAN(m)	10.7	-11.8	-27.3	0.9	1.6	-1.9	2.1	2.6	-8.5
STDEV(m)	7.6	8.9	17.3	7.5	8.7	13.6	8.8	6.0	7.9
MAX(m)	24.5	29.5	59.7	14.1	27.6	32.0	12.9	10.3	17.7
MIN(m)	0.5	0.1	0.3	0.1	0.1	0.6	1.1	0.4	5.4

As demonstrated in Figure 3 and Table 3, SECM achieves better result when more control points are used in triangulation. When the number of control points increases to 14, the MEAN of absolute errors achieves 1m level, which means that most of the systematic errors are eliminated. But the maximum residue is larger than 3 times of GSD (15m), so the SECM also cannot fit the real orbit and attitude of the satellite very well.

Triangulated Results of OIM with Different Control Strategies

To fully investigate the relationship between the number of GCPs used in triangulation and the residues of check points with OIM, 5 different control strategies (1), (2), (3), (4), and (5) are adopted.

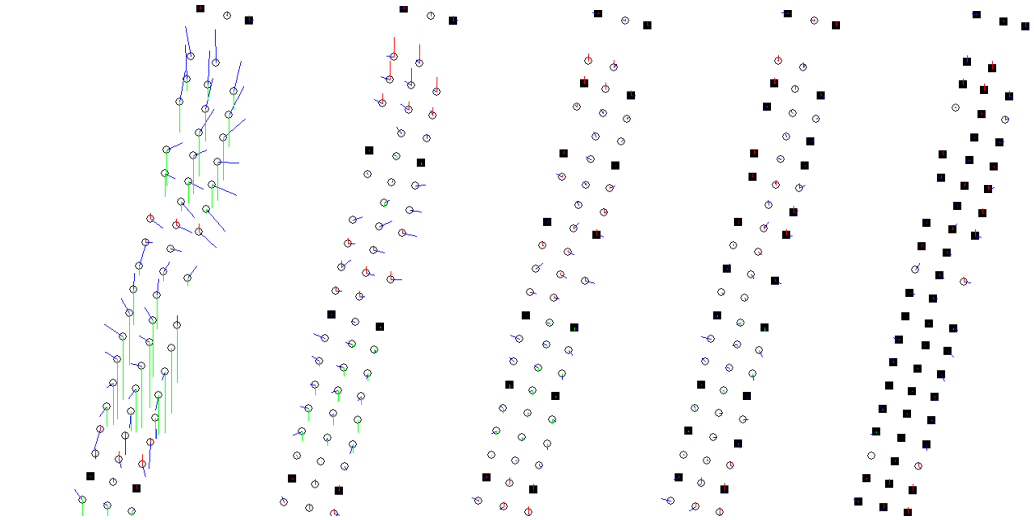

Figure 4. Absolute errors of control and check points of OIM (c) by control strategies (1), (2), (3), (4), (5).

Table 4. Error statistics of check points of triangulated results with OIM

CKPs RMS	4GCPs 54CKPs			8GCPs 54CKPs			14GCPs 44CKPs			22GCPs 36CKPs			52GCPs 6CKPs		
	X	Y	Z	X	Y	Z	X	Y	Z	X	Y	Z	X	Y	Z
MEAN	4.4	4.9	-34.9	-1.2	0.7	1.0	-0.4	0.5	1.0	-1.4	-0.1	1.5	3.9	1.8	3.7
STDEV	15.6	25.8	35.1	11.0	6.1	13.3	4.9	2.0	7.9	6.8	5.7	4.8	5.7	5.5	3.8
MAX	37.5	51.7	98.8	21.6	15.5	30.6	15.6	10.9	11.9	16.8	12.4	9.6	11.2	11.1	8.1
MIN	0.2	0.0	1.1	0.2	0.3	0.1	0.0	0.2	0.1	0.3	0.0	0.0	2.0	1.8	0.8

It can be seen from Figure 4 and Table 4 that the residues of CKPs become smaller as the number of GCPs increasing. But if there is only four GCPs, the residues of CKPs are quite large. The distribution of residues looks like waved lines. This is probably because four GCPs is not enough to control the whole orbit with longer than 1,000km distance. As the number gets to 14, the RMS of CKPs achieves about 5m horizontal and 8m vertical precision, respectively. The results of adjustment are slightly improved when more GCPs are used. The residues of control and check points in the five cases still look like waved lines, which means that the OIM is not precise enough to model the geometry of space-borne line CCD images.

CONCLUSION

Three models and 5 different control strategies are used for block adjustment with spaceborne three-line array dataset of 1,000km length orbit. The performance of QPM is worst, SECM is reasonable, and OIM is the best when appropriate control strategy (14 GCPs) is adopted. QPM and SECM are not suitable to model the positions and attitudes of long orbit satellite data. As control points increase, the accuracy of CKPs with OIM becomes higher. Acceptable results can be achieved with 14 GCPs. However, the improvement of adjusted results is not as significant as the increasing of GCPs.

15,000 scanning line is chosen as the interval of orientation images, and the weights of position and attitude data are fixed during adjustment. Further investigation will be made to test whether the used interval is suitable. Moreover, the weights of position and attitude observations also need to be re-evaluated after each iteration.

ACKNOWLEDGEMENTS

This work is supported by the National Natural Science Foundation of China with Project No. 41071233, and the Program for New Century Excellent Talents in University with Project No. NCET-07-0645.

REFERENCES

Ackermann, R., Bodechtel, J., Lanzl, F., Meissner, D., Seige, P., Winkenbach, H., 1990. MOMS-02 - A multi-spectral stereo imager for the second German Spacelab MissionD2, *Int. Arch. of Photogrammetry and Remote Sensing*, Vol. 28, Part 1, pp. 110-116.

Dial, Gene, Jacek Grodecki, 2002. Block adjustment with rational polynomial camera models, *ACSM-ASPRS 2002 Annual Conference Proceedings*.

Ebner, H., W. Konus, 1991a. Point determination using MOMS-02/D2 imagery, *Conference Proceedings IGARSS*, Helsinki 1991, Vol. III, pp. 1743-1746.

Ebner, H., O. Hofmann, W. Konus, R. Muller, G Stlunz, 1991b. A simulation study on point determination using MOMS-02/D2 imagery, *Photogrammetric Engineering & Remote Sensing*, Vol. 57, No. 10, pp. 1315-1320.

Ebner, H., W.Kornus, T. Ohlhof, 1992. A simulation study on point determination for the MOMS-02/D2 space project using an extended functional model, In: *Int. Arch. of Photogrammetry and Remote Sensing*, Vol. 29, Part B4, pp.458-464.

Gruen, A., S.Kocaman, K.Wolff, 2007. Calibration and validation of early ALOS/PRISM images, *The Journal of the Japan Society of Photogrammetry and Remote Sensing*, 46(1): 24-38.

Hofmann, O., Nav´e, P., Ebner H., 1982. DPS. A digital photogrammetric system for producing digital elevation models and orthophotos by means of linear array scanner imagery, *Int. Archives of Photogrammetry and Remote Sensing*, Vol. 24-III, 216-227, Helsinki, Finland, 1982.

Jung, W., J.S. Bethel., 2008. Stochastic modeling and triangulation for an airborne three line scanner, *The International Archives of the Photogrammetry, Remote Sensing and Spatial Information Sciences*. Vol. XXXVII. Part B1. Beijing 2008. pp. 653-656.

Kim, Taejung, Ian Dowman, 2006. Comparison of two physical sensor models for satellite images: position–rotation model and orbit–attitude model, *The Photogrammetric Record* 21(114): 110–123 (June 2006).

Kornus, W., et al. 2006. DEM generation from SPOT-5 3-fold along track stereoscopic imagery using auto calibration, *ISPRS Journal of Photogrammetry & Remote Sensing*, 60 (2006): 147-159.

McGlone, C., 1996. Sensor modeling in image registration, Digital Photogrammetry: An Addendum (C. W. Greve, editor), *American Society for Photogrammetry and Remote Sensing*, Bethesda, Maryland, pp. 115-123.

Ohlhof, T., 1995. Block triangulation using three-line images. *Proceedings of Photogrammetric Week 1995 (Wichmann, Verlag, editor)*, Stuttgart, pp, 197-206.

SPOT Image, 2002. SPOT Satellite Geometry Handbook, S-NT-73_12-SI, Edition 1, Revision 0, 15. 01. 2002.

Tao, C. Vincent, Yong Hu, 2001. A comprehensive study of the rational function model for photogrammetric processing, *Photogrammetric Engineering & Remote Sensing*, Vol. 67, No. 12, December 2001, pp. 1347-1357.

Yu, J., Yuan X., and Zhenli W, 2008. Calibration of constant angular error for CBERS-2 imagery with few ground control points, In: *The International Archives of Photogrammetry and Remote Sensing*, Vol. 37, Part B1, Beijing, pp. 769-774.

YUE Qing-xing, ZHOU Qiang, ZHANG Chun-ling, YOU Shu-cheng, JIA Yong-hong, QIU Zhen-ge, 2009. The adjustment of CBERS - 02B pan image, *Remote Sensing for Land & Resources*, Vol. 3, No. 1, pp. 61-63.

ZHAO Shuang-ming, LI De-Ren, 2006. Experimentation of adjustment math model for ADS40 sensor. *Acta Geodaetica et Cartographica Sinica*, Vol.35, No 4, Nov, 2006, pp. 342-346.